Removal of Inorganic Impurities in the Fast Pyrolysis Bio-oil Using Sorbents at Ambient Temperature

energy&fuels

pubs.acs.org/EF
Article

Removal of Inorganic Impurities in the Fast Pyrolysis Bio-oil Using Sorbents at Ambient Temperature

Emma Olsson Månsson, Abdenour Achour, Phuoc Hoang Ho, Prakhar Arora, Olov Öhrman, Derek Creaser, and Louise Olsson*

Cite This: *Energy Fuels* 2024, 38, 414–425

ABSTRACT: Fast pyrolysis bio-oil (FPBO) sourced from residual biomass waste (such as sawdust) is a promising feedstock that may be used for biofuel production. Their inorganic elements may, however, vary and cause deactivation of the catalysts in the hydrodeoxygenation (HDO) upgrading biorefinery unit. It was found that the use of zeolite Y and strong acidic ion-exchange resins as adsorbents was almost equally efficient in lowering the concentrations of Ca from <10 to <1 ppm and of Fe, K, and Mg to <0.3 ppm in FPBO at 30 °C, atmospheric pressure, and 4 h adsorption time. The removal efficiency of zeolite and resins exceeded 85−98% (detection limit) of these particular elements. For the first time for the FPBO, phosphorus was reported as being successfully targeted by aluminum oxide, being lowered from 1 ppm to <0.1 ppm, which is a reduction of at least 90%. Characterization of the oil and sorbents suggests that the surface acidity affects the removal efficiency of these elements from FPBO. Organic compounds in the pyrolysis oil, including isopropanol, lactic acid, hydroxy acetone, furfural, guaiacol, and levoglucosan, were semiquantified using two-dimensional gas chromatography coupled with mass spectrometry (GCxGC-MS). Compared to the fresh oil, the compositions and contents of these organic compounds were not impacted significantly by the sorbents under these mild operating conditions. This research indicates that inorganic impurities present in bio-oils can be removed, and thus, they may be considered feedstocks for producing biofuels with less deactivation of HDO catalysts.

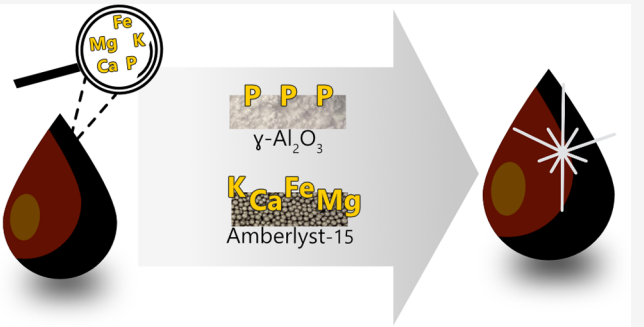

1. INTRODUCTION

The European Renewable Energy Directive (RED II) to reduce greenhouse gas (GHG) emissions, combined with the transition toward a fossil-free society, calls for the efficient use of alternative energy resources.[1] An increase in the amount of renewable biomass feedstock required for the production of fuel, without current land use being affected, is necessary to cover the demand as fossil-based fuels are being replaced.[2] Hydrogenated vegetable oils (HVOs) from industrial residues, such as tall oil from pulp and paper mills and waste cooking oil, give biofuels with lower carbon footprints and GHG emissions compared to conventional fossil-based fuels.[3,4] However, the challenge is that these are coproducts and are thereby constrained and limited to other processes.[5] It can therefore be argued that a widened accessibility of such feedstocks is important. Other solid industrial biomass residues from food and forestry production are being investigated, such as residues that can be converted to a liquid crude bio-oil by fast pyrolysis.[6−10] The crude fast pyrolysis bio-oil (FPBO) can be upgraded, which would enable the biofuel to be blended into the fossil fuel and be used in existing refineries and thereby facilitate a gradual replacement of fossil-based fuel.[11]

Successful coprocessing, together with petroleum intermediate products, requires the upgrading of bio-oils. Reducing the high water content, amounts of oxygenates, and acidity will improve its miscibility with other feedstocks and the stability of the bio-oil during storage.[11,12] The high content of oxygenated compounds (up to 49%)[13] found in the FPBO can be removed by catalytic hydrodeoxygenation (HDO) using catalysts such as sulfided NiMo supported on a high-surface area support such as aluminum oxide.[2,14−16] The HDO for bio-oils has been widely studied in recent years, and feedstocks such as FPBO are particularly challenging for commercial applications. It has been studied as both a direct and two-step process, with either conditions close to 300−350 °C and up to 100 bar H_2 pressure depending on the feedstock or a mild hydrogenation at 200 °C, followed by deep hydrogenation at 350 °C.[12] Catalyst deactivation caused by coking of Ni-, Mo-, and Pt (or

Received: July 7, 2023
Revised: November 19, 2023
Accepted: November 28, 2023
Published: December 18, 2023

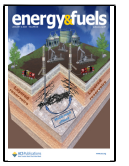

https://doi.org/10.1021/acs.energyfuels.3c02473
Energy Fuels 2024, 38, 414−425

bimetallic)-promoted materials is a known problem, which is studied using the FPBO and model compounds such as oleic acids or pure vegetable oils such as palm oil.[17−19] In this paper, the focus is on the deactivation caused by inorganic compounds from a more complex feedstock such as FPBO.

Olarte et al.[14] found that a plug of polymerized bio-oil and inorganics covering the catalysts prevented the liquid and gas from flowing through the bed, resulting in a shutdown due to pressure excursion. They studied the effect of a pretreatment stage before the HDO that could prevent these issues from arising due to the unstable nature of the FPBO. Although a pretreatment, comparing 80 and 140 °C using Ru on high-surface area carbon as the catalyst, prevented the formation of a solid plug, a loss in surface area was shown that led to deactivation. Arora et al.[20,21] studied this deactivation more closely using iron stearate, a phospholipid, and potassium nitrate to represent known poisons to the HDO catalysts MoS_2 and sulfided NiMo on Al_2O_3. They reported that Fe had a large impact even at low concentrations and that phospholipids resulted in a decreased surface area, pore volume, and pore size distribution effects. K and P can be found, in varying amounts, in residual industrial biomasses, such as bark and sawdust from sawmills. Fe can be corroded from the steel storage tanks by the acidity of the oil. It is therefore important that these impurities are removed to reduce catalyst deactivation in the upgrading process.[20] To overcome such catalyst deactivation, a guard bed is commonly used in fossil refineries for the selective removal of unwanted impurities. The guard bed can, e.g., be a column with multiple packed beds with robust, low-performance catalysts that remove poisonous organic and inorganic compounds from the oil.[22−24] The treated oil can then be upgraded further with fewer costly shutdowns induced by catalyst deactivation.

Demetallization and the removal of alkalis and other inorganic elements by adsorption are well-established processes found in existing petroleum refineries,[25] wastewater treatment,[26,27] and plastic recycling processes.[28] Adsorbents reported as being able to capture alkali and alkali earth metals, heavy metals, transition metals, and half-metals are aluminum oxides,[20,27] zeolites,[15,24,29] activated carbon,[25,30,31] and ion-exchange resins.[32] These adsorbents and ion-exchangers show a high adsorption capacity and a regeneration rate, making them suitable for industrial applications.[26,27] The removal of impurities found in the FPBO that are poisonous to catalysts is an important direction for future research, as described by Oasmaa et al. and Arora et al.[12,21] To the best of our knowledge, there is only one study pertaining to the removal of inorganic cations in real pyrolysis oils. Zhou and Roby[32] used strongly acidic cation-exchange resins, such as Amberlyst, to remove metal cations in solvent-diluted pyrolysis oils with a high inorganic content that were assumed to be in an ionic form. The aim of the solvent was to reduce the kinematic viscosity and homogenize the oil at ambient temperatures and isopropanol (2-propanol) at 15−30 wt % was found to be appropriate. They reported successful reduction to <5 ppm, finding that the rate followed the sequence $Na^+ > K^+ > Mg^{2+} > Ca^{2+} \gg Fe^{3+}$, and concluded that further studies are required pertaining to the complexity of the systems and the removal of multivalent ions.[32]

No research studies have been published concerning the removal efficiency of low concentrations of both cationic metals and multivalent ions such as phosphorus in FPBO, which is the aim of the current work. Also, there are no studies that have investigated whether resins and other adsorbent materials influence the chemical composition of the pyrolysis oil. The objective here is therefore to study the selective removal of the HDO catalyst poisons Ca, Fe, Mg, K, and P from the pyrolysis bio-oil produced from residual sawdust. Zeolite, aluminum oxide, and different acidic resins are compared at ambient conditions. This paper also includes a semiquantification of common organic compounds found in the pyrolysis bio-oil to examine the impact the absorption process may have, if any, on the bio-oil chemical composition.

2. EXPERIMENTAL SECTION

2.1. Materials. FPBO was supplied by Preem AB (Sweden) and produced from softwood sawdust of Nordic origin. Absolute ethanol (99.99%, Sigma-Aldrich) and nitric acid (68%, Sigma-Aldrich) were used as received or diluted with Milli-Q water. The sorbents used were Amberlyst 15 in a dry hydrogen form (Sigma-Aldrich, Sweden), protonated Dowex 50WX8 (Dowex 8) and 50WX2 (Dowex 2) both in a gel form with 50/100 mesh size (Sigma-Aldrich), zeolite Y (USY) CBV-712 (Zeolyst), and aluminum oxide (γ-Al_2O_3) (Puralox SBa 200, Sasol). All of the resins swell on contact with a liquid.

The sorbents γ-Al_2O_3 and USY were calcined at 550 °C for 4 h, with a heating ramp of 5 °C min^{-1}. Amberlyst was used as received, while Dowex 2 and Dowex 8 were both dried overnight at 85 and 110 °C, respectively.

The glassware used in the experiments was washed and dried in an oven at 80 °C. The perfluoroalkoxy (PFA) vials and magnets for stirring were sterilized using nitric acid diluted to 7% for 4 h and dried in an oven at 80 °C between the runs. 30 mL glass crucible filters of pore sizes of 16−45 μm (Robu glass) were used to separate the sorbents from the oil after the experiment.

2.2. Adsorption Experiments to Remove Inorganic Impurities. Experiments were carried out in 30 mL inert PFA vials with the highest resistance to chemicals and sealed with a PFA screw cap (WVR), and glass crucible filters were used for filtration.

The adsorption experiments were conducted in batches using washed PFA vials. The sorbent concentration (5−10 wt % relative to the oil) was compared for the five sorbents. The experiments with 10 wt % sorbent were repeated, and the average of the experiments is shown in the results. The repetitions were made close in time using the same batch of oil. Variations for repeated ICP analysis of the fresh pyrolysis oil (see Table S1) were ±0.28 for Ca and < ± 0.06 for Fe, K, Mg, and P. When the concentrations are below 1 ppm, there are some differences in the repetitions, which are due to the very low level, close to the detection limit (Table S2). A vial was loaded with 26 g of the oil, 5 or 10 wt % of the sorbent, and 10 wt % of ethanol (relative to the oil). The ethanol was added to reduce the viscosity and thus enable the adsorption process at ambient temperature in our laboratory experiments and simultaneously improve the liquid−solid mass transfer, as studied elsewhere for FPBOs.[32,33] Another method for reducing the viscosity could have been increasing the temperature, but this is not possible since higher temperatures will speed up the self-polymerization of the oil. A magnet was inserted in the vial before it was placed in a sand bath, which maintained a homogenous temperature of 30 °C, and stirred at 1000 rpm for 4 h. The slurry was then separated into solid and liquid fractions by using a glass filter crucible and a vacuum pump. An additional 10 mL of ethanol was added in the filter crucible to facilitate the filtration. Once the oil filtrate was collected, the sorbents were rinsed with additional ethanol, until all excess oil was removed. The filter crucibles with the sorbents were dried overnight at 80 °C and then collected, Figure 1.

2.3. Characterization of the Oil and Sorbent. A Karl Fischer 870 Titrino Plus, Metrohm, was used to determine the water content in the FPBO thus: a small sample of oil was injected into the glass chamber filled with Hydranal (Honeywell Fluka) and titrated automatically using Karl Fischer titrant composite 5 (Honeywell Fluka). The procedure was repeated twice, and the average value was used.

https://doi.org/10.1021/acs.energyfuels.3c02473
Energy Fuels 2024, 38, 414−425

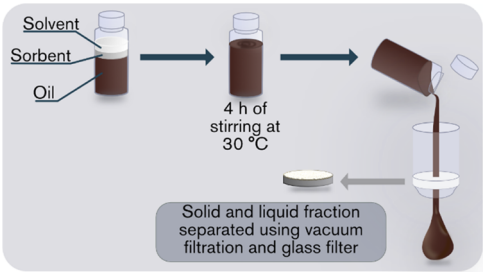

Figure 1. Adsorption experiment setup.

The total acid number (TAN) of the FPBO was determined by automatic titration using an Orion Star T910 with a pH probe according to a modified ASTM D664 method. The modified method developed by Agblevor et al.[34] used aqueous KOH (45 wt % in water) diluted to 0.1 M in Milli-Q water as a titrant and acetone as the titration solvent (Sigma-Aldrich). A 0.1 g amount of bio-oil sample was added to 50 mL of acetone, and KOH was titrated until the pH reached 11. TAN (mg of KOH g of oil^{-1}) was calculated using the difference in KOH volume (mL) added between the real and a blank sample, the concentration of the KOH solution, N_{KOH} (mmol mL^{-1}), the molecular weight of KOH, M_{KOH} (mg mmol^{-1}), and the sample weight (g), presented in eq 1. The procedure was repeated three times for both the blank and the fresh oil sample, and the average value was used.

$$\text{TAN} = \frac{V_{\text{KOH(real-blank)}} \cdot N_{\text{KOH}} \cdot M_{\text{KOH}}}{\text{sample weight}} \quad (1)$$

The density and viscosity (ASTM D5002−22 and D445−21e2, respectively) of the fresh oil were measured using Anton Paar equipment (DMA 4500 M and SVM 3001, respectively). The fresh oil was also characterized using thermogravimetric analysis (TGA/DSC3+ Star system, Mettler Toledo) from room temperature up to 800 °C at 10 °C min^{-1} under a gas flow rate (air or N_2) of 60 mL min^{-1}. The elemental composition of the FPBO was carried out by elemental microanalysis (Devon, U.K.) using the Dumas combustion method for C, H, N, and S and Unterzaucher pyrolysis for O. The higher heating value (HHV) in MJ kg^{-1} was calculated employing Dulong's formula (eq 2) using the elemental compositions obtained (wt %) of carbon, hydrogen, and oxygen for the FPBO in the dry form[35]

$$\text{HHV} = 0.3383\text{C} + 1.442 \cdot \left(\text{H} - \frac{\text{O}}{8}\right) \quad (2)$$

The elemental impurities in the fresh and purified FPBO and spent sorbent material were measured using inductively coupled plasma with sector field mass spectrometry (ICP-SFMS) (ALS Scandinavia AB, Luleå, Sweden) according to SS EN ISO 17294−2:2016 and the EPA method 200.8:1994. The oil was digested using HNO_3, and the sorbent material was digested using lithium metaborate fusion (ASTM D3682:2013; ASTM D4503). Concentrations of the elements Ca, Fe, Mg, K, and P are given in parts per million in weight mg kg^{-1}, hereafter referred to as ppm, with detection limits of 1 0.02, 0.1, 0.1, and 0.1 ppm, respectively, in the FPBO. In the sorbent material, the detection limits were reported at 20 0.08, 0.01, 0.04, and 1 ppm. The concentrations of impurities on the sorbent material of each element j (c_j) in mg kg^{-1} were converted to absolute mass (m_j) using the mass of the sorbent and oil used in the experiments ($m_{\text{sorbent,exp}}$, $m_{\text{oil,exp}}$) according to the equations given below

$$m_{j,\text{sorbent,exp}}[\text{mg}] = c_j[\text{mgkg}^{-1}] \cdot m_{\text{sorbent,exp}}[\text{kg}] \quad (3)$$

$$m_{j,\text{oil,exp}}[\text{mg}] = c_j[\text{mgkg}^{-1}] \cdot m_{\text{oil,exp}}[\text{kg}] \quad (4)$$

The removal efficiency of each element was calculated using their initial (C_0) and final (C_f) concentrations in the oil in ppm measured by ICP (eq 3). The calculation accounted for the ethanol added during the experiments; the dilution factor yields an offset of about 25% of the detection limits as indicated in the plots.

$$\text{removal efficiency (\%)} = 100 \cdot \frac{C_0 - C_f}{C_0} \quad (5)$$

Scanning electron microscopy (SEM) was used for size and shape identification (Zeiss). The Brunauer−Emmett−Teller (BET) method was used for calculating the BET specific surface area (Micromeritics Tristar 3000) for USY and γ-Al_2O_3 by degassing approximately 200 mg of sorbent at 90 °C for 1 h and then at 300 °C for 3.5 h, followed by nitrogen sorption at 77 K. Ammonia temperature-programmed desorption (NH_3-TPD) was conducted to measure surface acidity: about 30 mg of sorbent, pelletized, and sieved to a fraction of 180−250 μm was added to the differential scanning calorimeter (Sensys DSC, Setaram), where the gas flow of pure Ar and NH_3 in Ar was regulated using mass flow controllers (MFC, Bronkhorst) and coupled to a mass spectrometer (HPR-20 QUI, Hiden) for monitoring the outlet NH_3 (mass signal m/z = 17). The sample was first treated with pure Ar at 300 °C for 30 min and then cooled to 100 °C. NH_3 was introduced to the reactor at a concentration of 2000 ppm, balanced with Ar, at a flow of 20 mL min^{-1} for 90 min to fully saturate the sample. Flushing with pure Ar for 60 min thereafter removed the physisorbed NH_3. Desorption was then performed while increasing the temperature from 100 to 700 °C at a ramp rate of 10 °C min^{-1}.

The fresh and pretreated oils were analyzed using comprehensive two-dimensional gas chromatography (GCxGC, Agilent 7890B) equipped with a midpolar column (VF-1701MS, 30 m × 250 μm × 0.25 μm), nonpolar DB-5MS (3.0 m × 150 μm × 0.15 μm) column, and mass spectrometry detector (MSD, Agilent 5977A). The injector temperature was set at 280 °C, and helium was used as the carrier gas at a flow of 0.8 and 1.0 mL min^{-1} for the first and second columns, respectively. The oven temperature was kept initially at 40 °C for 1 min before being ramped to 280 °C at a rate of 2 °C min^{-1}. The thermal modulation was kept at 4 s for all of the samples. Dihexyl ether (Sigma-Aldrich) was added as an internal standard (IS), and the amount of solvent was constant in both the fresh and experimented samples at 10 wt % relative to the oil. Agilent software (GC Image version 2.9 GCxGC) was used to identify and integrate peak volumes,

Table 1. Properties, Elemental Composition, and Inorganic Content of the FPBO

properties		elemental composition	wt %	inorganic content	ppm
water (%)	23.0 ± 0.2	C[d]	43.8 ± 0.2	Ca	9.2 ± 0.3
pH	2.5−3.5	O[d]	26.6 ± 0.8	Fe	1.7 ± 0.04
TAN (mg KOH g^{-1})	109 ± 6	H[d]	4.71 ± 0.1	K	5.1 ± 0.06
density[a] (kg dm^{-3})	1.19	N	0.11 ± 0.001	Mg	1.8 ± 0.02
viscosity[b,c] (cSt)	32	S	<0.1 ± 0.001	P	0.93 ± 0.014
HHV (MJ kg^{-1})	16.8	ash content[e]	0.03		
		H/C[d,f]	1.3		
		O/C[d,f]	0.46		

[a]at 15 °C. [b]at 40 °C; [c]kinematic. [d]dry. [e]after air flow. [f]atomic.

https://doi.org/10.1021/acs.energyfuels.3c02473
Energy Fuels 2024, 38, 414−425

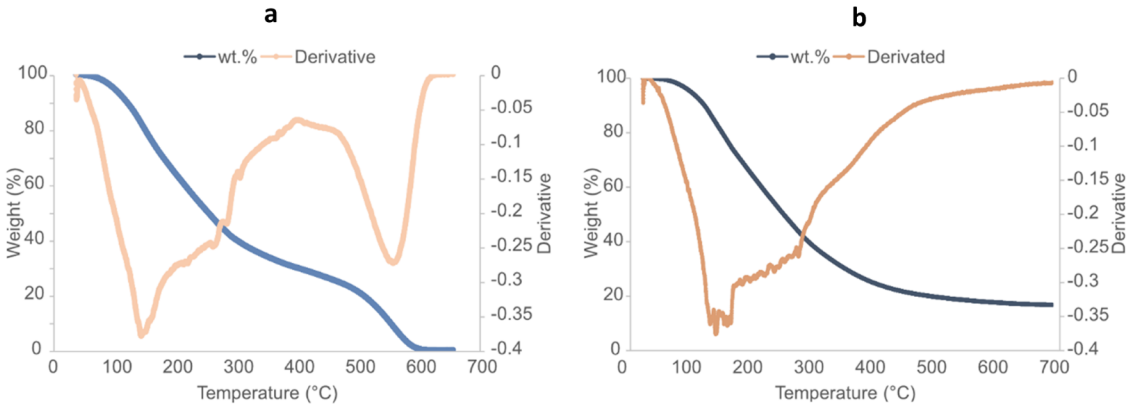

Figure 2. Thermogravimetric analysis (TGA) and derivatized TG curves for the FPBO during air (a) and N_2 flow (b).

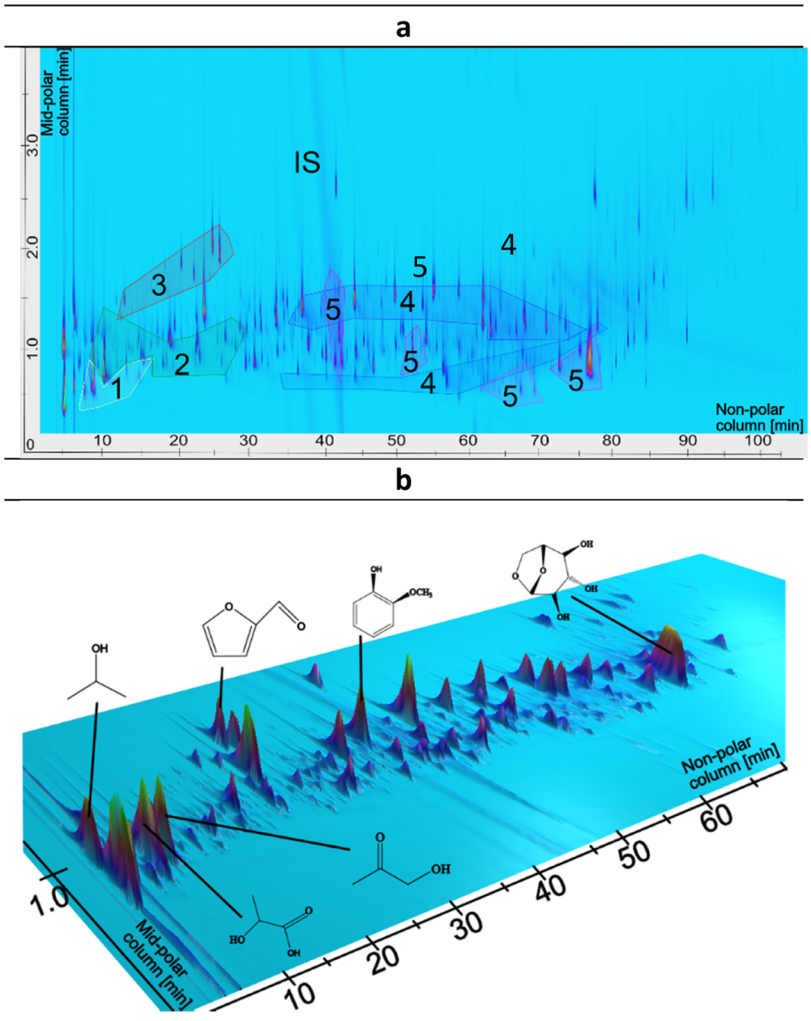

Figure 3. GCxGC-MS spectra of fresh FPBO with 10 wt % added EtOH and internal standard (IS). (a) 2D plot of the functional groups: (1) acids, (2) ketones and aldehydes, (3) furans, (4) phenols, and (5) sugars. (b) 3D plot of the spectra: (from left to right) isopropanol, lactic acid, hydroxy acetone, furfural, guaiacol, and levoglucosan.

which were compared among the samples to estimate changes within typical compounds. The peak spectra identified were compared to those in the NIST library.

3. RESULTS AND DISCUSSION

3.1. FPBO Characterization. The properties of the FPBO (Table 1) lie within the averages of the typical properties of a FPBO, presented in parentheses, for water content (20−30 wt %), pH (2−3), density (1.1−1.3 kg dm^{-3}), and viscosity (15−35 cSt).[36] The TAN in this sample (109 mg KOH/g) is comparable to that of the wood-based pyrolysis oils in the literature reported at an average of 97.[37,38] The inorganic elements investigated were present in the fresh oil, with their concentration decreasing in the order Ca > K > Mg > Fe > P >

https://doi.org/10.1021/acs.energyfuels.3c02473
Energy Fuels 2024, 38, 414−425

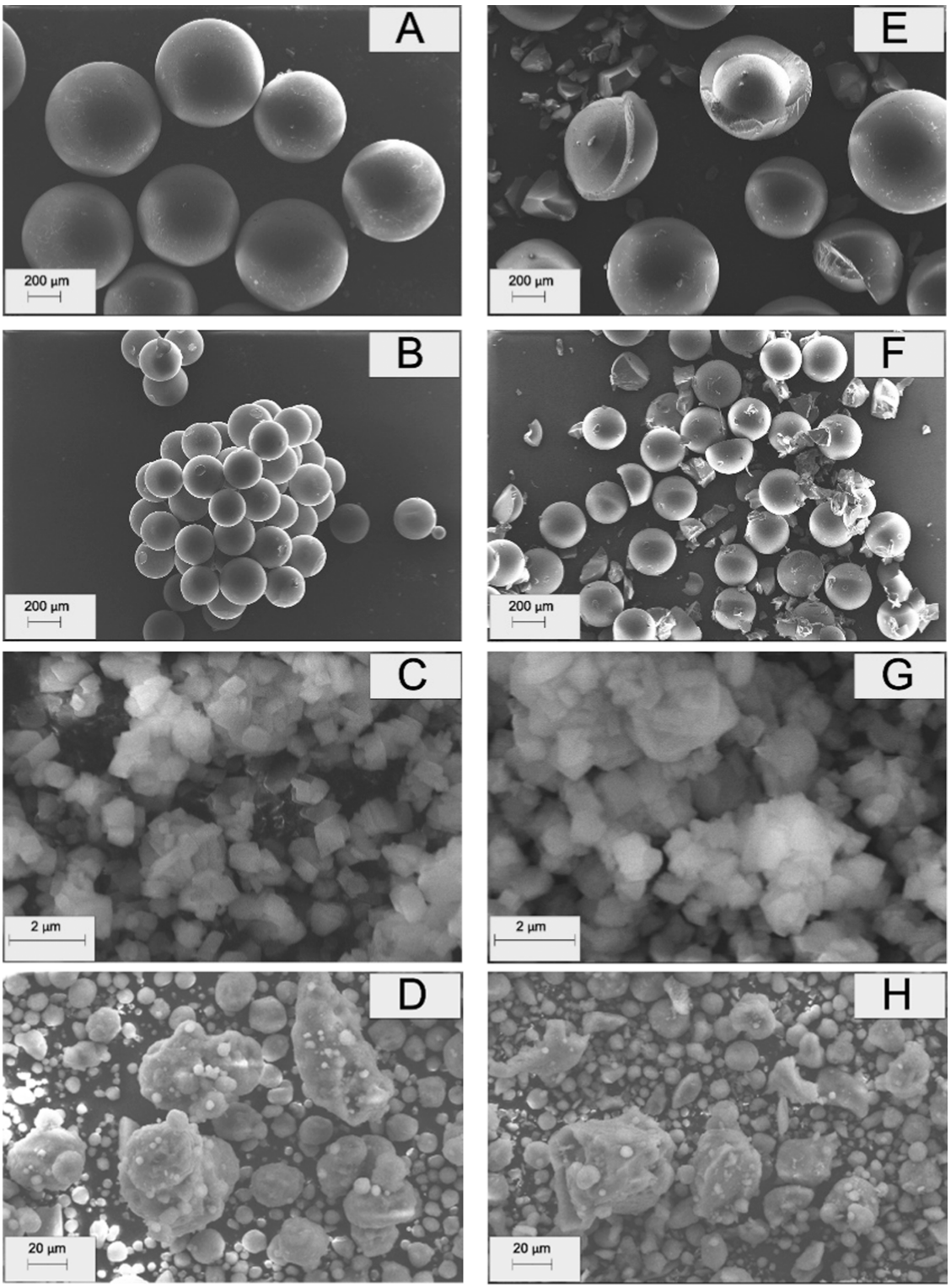

Figure 4. SEM images of fresh Amberlyst (A), Dowex 2 (B), USY (C), and γ-Al_2O_3 (D) and those after the experiment (E−H).

Na and ranging from 9.2 to 0.55 ppm, based on an average of two samples.

TGA was performed on the fresh FPBO using either air (Figure 2a) or N_2 (Figure 2b) flow, primarily to discover the starting temperature of devolatilization and thus the experimental limit of this study. The initial devolatilization of the FPBO began at 45−50 °C under air (Figure 2a). The maximum rates of change during combustion were found at around 150 and 550 °C, which can be seen by examining the derivatized thermogravimetric (DTG) curve. The ash content was determined as the residual mass when there was no change in mass during oxidation: this occurred at temperatures higher than 600 °C and resulted in an ash content of 0.03 wt %. The boiling points and degree of volatility both suggest that residual water, acids, ketones, or furans are converted/evaporated early on at around 150 °C, while larger and more

https://doi.org/10.1021/acs.energyfuels.3c02473
Energy Fuels 2024, 38, 414−425

complex structures are converted at around 550 °C. TGA under inert N_2 conditions (Figure 2b) confirms the evaporation of volatile compounds at 150 °C, but no peak at 550 °C was observed: this could be due to that anhydrosugars (such as levoglucosan) form char[39] or the secondary reactions of lignin-derived components (reported at 425−570 °C)[40] that were combusted in the presence of oxygen.[39]

FPBO is composed of hundreds of compounds with varying volatility, polarity, and molecular weights: typical compositions vary, depending on the pyrolysis method and feedstock used. The most abundant compound group present in FPBOs is hydroxyls, which include carboxylic acids (4−15 wt %), phenolics (17−35 wt %), sugars (20−35 wt %), and water (20−30 wt %).[41,42] GCxGC-MS analysis provided information regarding the monomeric fraction present in the FPBO, including volatile and semivolatile compounds. The average molecular weight of FPBO produced from sawdust 554 g mol^{-1} (an average reported on a FPBO sample of the same feedstock from the same producer by gel permeation chromatography using tetrahydrofuran (THF) as a mobile phase)[43] indicates the presence of large compounds. Although extensive characterization of bio-oils and method development of GCxGC analysis have been reported for FPBOs in the literature, variations in the biomass feedstock, the pyrolysis process and GC analysis methods, and precision make comparing results challenging.[44−46] Therefore, in this paper, some typical functional groups have been categorized by GCxGC analysis (marked 1−5 in Figure 3a), and a few of the most typical compounds were selected in these groups, namely, isopropanol, lactic acid (1), hydroxy acetone (2), furfural (3), guaiacol (4), and levoglucosan (5); their chemical structures and peaks are shown in Figure 3b. These have been semiquantified and compared after the adsorption experiments presented later in the present study.

3.2. Sorbent Characterization. SEM images show that prior to the adsorption, the spherical resin particles have a smooth surface with diameters of 600 and 100 μm for dried Amberlyst and Dowex resins, respectively (Figure 4A,B). In the dried state, the Dowex resins show up as clusters of about 800 μm. Those of USY and γ-Al_2O_3 were both significantly smaller: 1 and up to 10 μm, respectively. After 4 h of the adsorption removal experiment (Figure 4E,F), the spherical resin particles collapsed into fractured particles, whereas exposing the resin to the FPBO for a prolonged period of time but without any stirring did not result in any fracturing occurring. These results suggest that the resins were degraded by shear force/attrition due to magnetic stirring rather than chemical degradation caused by acidic FPBO. USY and γ-Al_2O_3 did not seem to be affected by attrition. The USY is an ultrastable type of Y-zeolite known for maintaining its structure even under harsh reaction conditions, likely due to the mild dealumination treatment it undergoes during production.[47] The γ-Al_2O_3 is a common catalytic support material used, e.g., during catalytic hydrotreatment of bio-oils that is carried out under high temperatures and pressures.[15]

The specific BET surface area of USY was 643.3 m^2 g^{-1} and that of γ-Al_2O_3 was lower at 195.9 m^2 g^{-1}. BET and NH_3-TPD were not measured for the resin materials due to their heat-sensitive nature. The resins also expand in contact with liquids and thereby increase in surface area.[48] Their dried surface area obtained using a BET instrument would not be representative of the experimental conditions here. The acidic properties of USY and γ-Al_2O_3 were studied using NH_3-TPD: the profiles of both samples (Figure S1 in the Supporting Information) show two pronounced peaks, indicating the presence of weak (at approximately 350 °C) and strong acid sites (at approximately 375 °C). The quantification of the NH_3-TPD data is presented in Table 2; the raw data can be found in Figure S1 in the Supporting Information.

Table 2. Average Particle Size, BET Surface Area, and Acidity of the Fresh Sorbent Materials

	average size (μm)	BET surface area (m^2 g^{-1})	acidity (μmol NH_3 g^{-1})
USY	1	643.3 ± 14.4	774.1
γ-Al	1−10	195.9 ± 0.34	317.5
DWX	200−250		
AMB	300		2140[49]

The concentrations of inorganics present in each adsorbent prior to experiments are shown in Figure 5. The results show

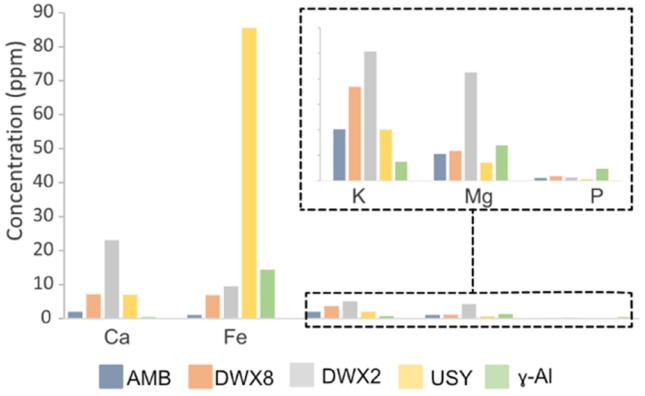

Figure 5. Concentration of impurities in each fresh sorbent material at 0−6 ppm (a) and 0−90 ppm (b), measured by ICP-SFMS.

that the concentrations of Fe in USY (85.5 ppm) and Ca and Mg in Dowex 2 (23.1 and 4.25 ppm, respectively) are higher than that of the FPBO (1.8, 8.85, and 1.89 ppm, respectively). This presents a risk that inorganics could, in some cases, be released from the sorbent to the oil. However, this depends not only on the concentration of the inorganic substance in the sorbent but also on its binding strength. Naturally occurring iron (Fe) in USY is present in the highest concentration, while all of the other elements are below 25 ppm. Phosphorus (P) has the highest concentration in γ-Al_2O_3 (~0.5 ppm), but it is still very low and is even lower in the other sorbents (<0.18 ppm). The concentrations of potassium (K), magnesium (Mg), and calcium (Ca) in the resins were generally higher in the Dowex resins and lower in Amberlyst and lower in Dowex 8 (3.7, 1.2, and 7 ppm, respectively) than in Dowex 2 (5, 4, and 23 ppm, respectively). The reason for this could be that the strength or crosslinking (8 vs 2%) differs between the two Dowex resins. Based on ICP measurements, the Si/Al molar ratio for USY was close up to 7.

3.3. Removal of Impurities by Adsorption. A previously reported study targeted and reduced cations using resins from initial levels of 620, 138, 616, and 29 ppm for K^+, Mg^{2+}, Ca^{2+}, and Fe^{3+}, respectively, to lower than 5 ppm after 24 h using a mechanical shaker at ambient conditions.[32] The FPBO in that particular study was sourced from hardwood and diluted with isopropanol to reduce the kinematic viscosity from >400 to

https://doi.org/10.1021/acs.energyfuels.3c02473
Energy Fuels 2024, 38, 414−425

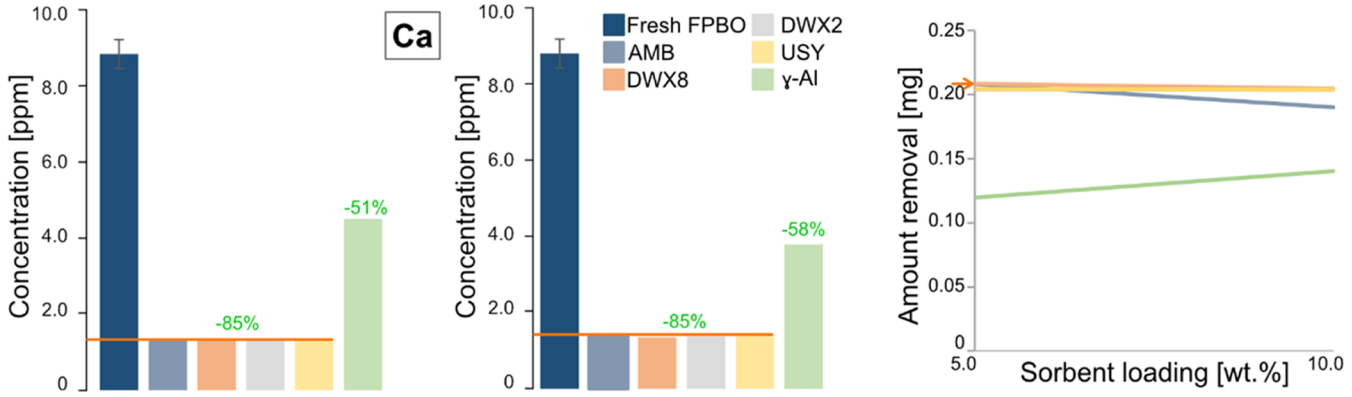

Figure 6. Concentration of Ca in ppm in the FPBO at sorbent loadings of 5 (a) and 10 wt % (b), comparing the fresh content for all five sorbent experiments. (c) Total amounts of Ca removed (in mg) for (a, b). The orange line in (a, b) panels denotes the detection limit.

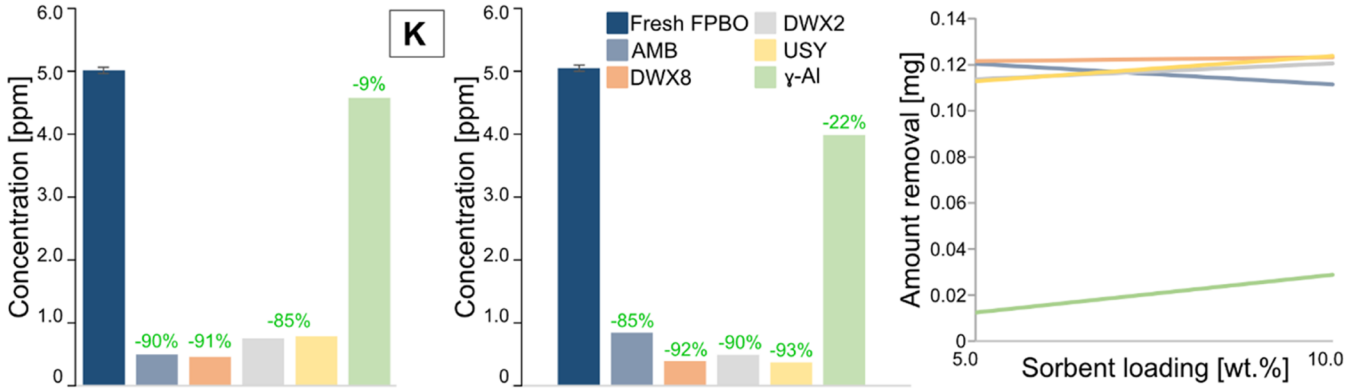

Figure 7. Concentration of K in ppm in the FPBO at sorbent loadings of 5 wt % (a) and 10 wt % (b), comparing the fresh content for all five sorbent experiments. Total amounts of K removed (in mg) for (a, b) are shown in (c).

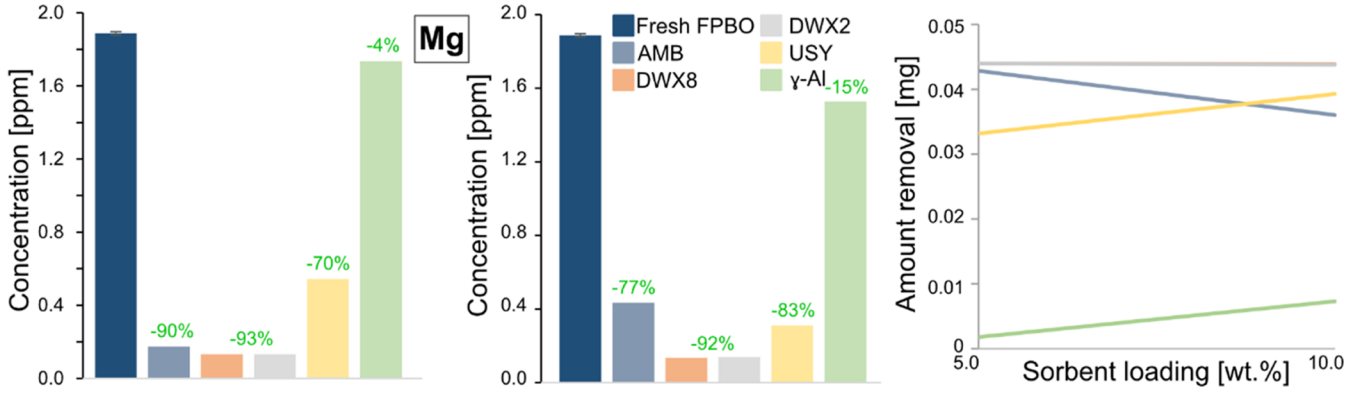

Figure 8. Concentration of Mg in ppm in the FPBO at sorbent loadings of 5 (a) and 10 wt % (b), comparing the fresh content for all five sorbent experiments. Total amounts of Mg removed (in mg) for (a, b) are shown in (c). The orange line in (a, b) panels denotes the detection limit.

<60 mm^2 s^{-1}. The criteria in the literature were that an ideal organic solvent must be miscible with FPBO, result in no chemical reaction with FPBO, no negative consequences on the refinery process, and lower viscosity, have low volatility, and be cost efficient, environmentally friendly, safe to handle, and recyclable.[32]

In the present study, the concentrations of the initial impurities were significantly lower (<10 ppm for all elements, an average of two fresh FPBO samples plotted in Figures 6−10 are presented in Table S1 in SI). After the adsorption process, these were reduced to <1 ppm for Ca (Figure 6), < 0.4 ppm for K (Figure 7), and <0.2 for Mg (Figure 8), Fe (Figure 9), and P (Figure 10) after 4 h using a magnetic stirrer. Due to the very low amount of Na in the fresh oil (0.55 ppm, Table 1), it was difficult to obtain reliable results regarding its removal and is therefore not included here. The reproducibility was evaluated with different sorbent loadings and FPBO of different batches. Additional experiments were repeated for Amberlyst and γ-Al_2O_3, which can be found in the Supporting Information, Table S3−S4 and Figure S3, which showed variations of ± <0.2 ppm for Amberlyst and the variation was ± <0.1 ppm for γ-Al_2O_3.

The effect of using 5 or 10 wt % of adsorbents is compared for each component. It can be noted that the orange line and

https://doi.org/10.1021/acs.energyfuels.3c02473
Energy Fuels 2024, 38, 414−425

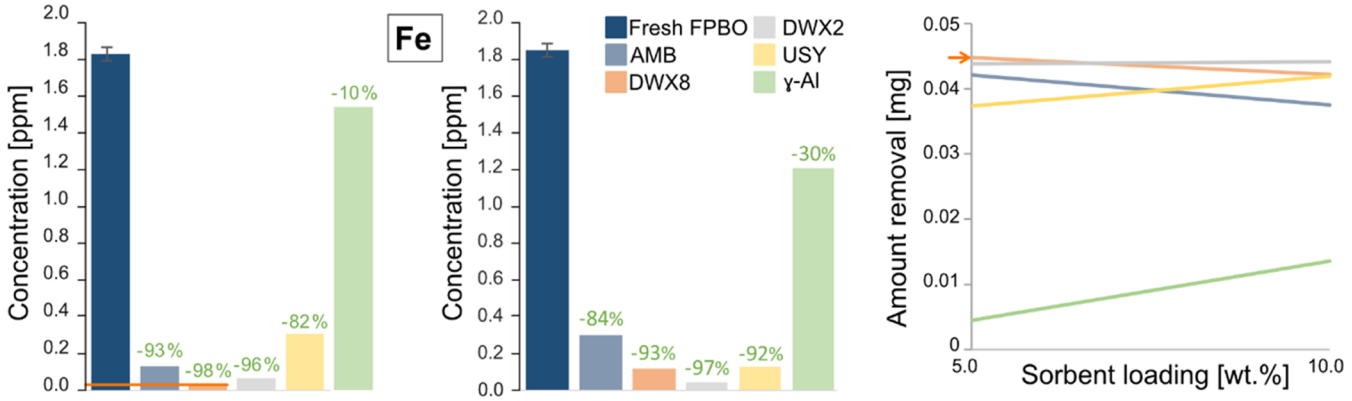

Figure 9. Concentration of Fe in ppm in the FPBO at sorbent loadings of 5 wt % (a) and 10 wt % (b), comparing the fresh content for all five sorbent experiments. Total amounts of Fe removed (in mg) for (a, b) are shown in (c). The orange line in (a) denotes the detection limit.

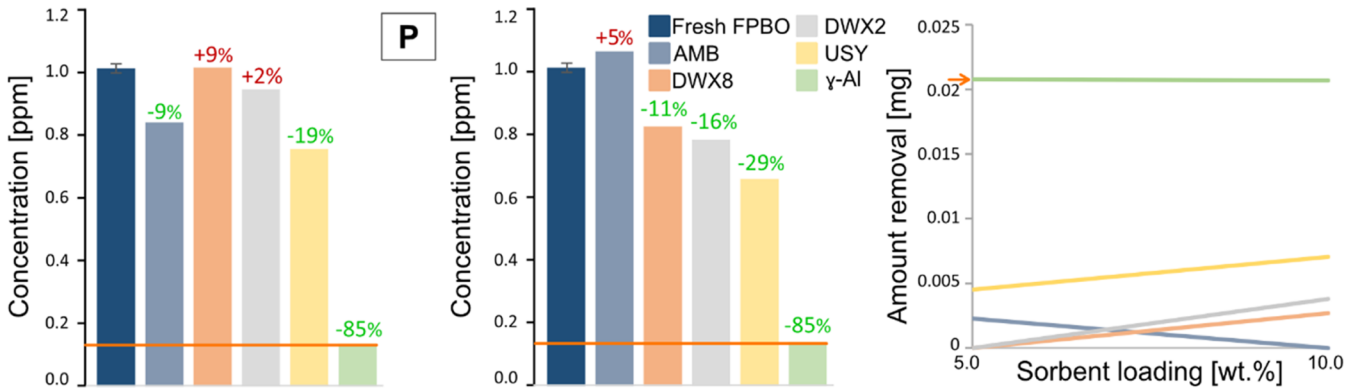

Figure 10. Concentration of P in ppm in the FPBO at sorbent loadings of 5 wt % (a) and 10 wt % (b), comparing the fresh content for all five sorbent experiments. Total amounts of P removed (in mg) for (a, b) are shown in (c). The orange line in (a, b) denotes the detection limit.

arrow displayed in Figures 6,8,9 and 10 mark the detection limit (DL) for that component, so the actual concentration could have been even lower. The removal of inorganic elements increased when the sorbent loading was increased from 5 to 10 wt % relative to the oil, albeit to a small extent. This can be seen by comparing the results in (a) with those in (b), which are also plotted in actual mass (in mg) in (c) (Figures 6–10c). The increase in sorption is expected when the amount of the adsorbent is increased because more adsorption sites become available. For removal below the detection limit, however, there is no difference between 5 and 10 wt % (as for the USY and resins with Ca shown in Figure 6). In the case of Amberlyst, the removal was less efficient for P, K, and Mg when increasing the sorbent loading and thus available sites. This was unexpected and did not occur for any of the other sorbents. The experiment with the Amberlyst sorbent was repeated (using the same FPBO in Table S2 and a new batch of the FPBO in Tables S3 and S4), and variations of ±0.3 ppm (but often much lower) were seen at these very low levels. The repeated experiments with Amberlyst indicated that there was a larger standard deviation at 5 wt % but that the removal did in fact increase when increasing the sorbent loading for Ca, Fe, and Mg. It did not seem to affect P removal, and for K, the average concentrations suggested that its removal was greater at 5 wt % than at 10 wt %, although the error bars did overlap. The main property differing from the Amberlyst from the other sorbents (which did not present this trend) is the size, which was significantly larger for the Amberlyst compared with the others (Figure 4). It should also be noted that the final concentrations for all elements after Amberlyst adsorption experiments were below 1 ppm; thus, it is also possible that these small variations are due to the fact that the low concentrations are too close to the detection limit of the ICP-SFMS analysis.

The resins and USY were successful in removing the cationic species Ca, K, Mg, and Fe, where Ca, Mg, and Fe were even removed below their corresponding detection limits (i.e., removal of at least 85, 93, and 98%, respectively). Also, K was removed most at 90–91% using these sorbents. Compared to γ-Al_2O_3, they removed (at least) almost twice as much Ca and up to 10-fold more K, Mg, and Fe. The resins have strong Brønsted acid sites due to the sulfonic acid ($-HSO_3$) exchanging group, which dissociates $(-SO_3)^-$ and H^+.[49] Moreover, the USY is well known for having a high Brønsted acidity.[50] On the other hand, γ-Al_2O_3 has a lower total acidity compared to the USY (Table 2), with the acidity being mostly Lewis acidity.[50] This could explain why the resins and USY have significantly higher removals of Ca, K, Mg, and Fe. Overall, it was the strongly acidic ion-exchange resin Dowex 8, closely followed by Dowex 2 and Amberlyst, that were most successful in removing all the cations Ca, K, Mg, and Fe.

The opposite trend was observed in the removal of the multivalent ion P, with successful removal only by γ-Al_2O_3, while the strongly acidic sorbents showed no effect. It was removed below the detection limit (85%), which corresponds to a detection level of 0.1 ppm. Yang et al.[51] studied and compared two types of aluminum oxides for phosphate adsorption from an aqueous solution of KH_2PO_4 to simulate

https://doi.org/10.1021/acs.energyfuels.3c02473
Energy Fuels 2024, 38, 414–425

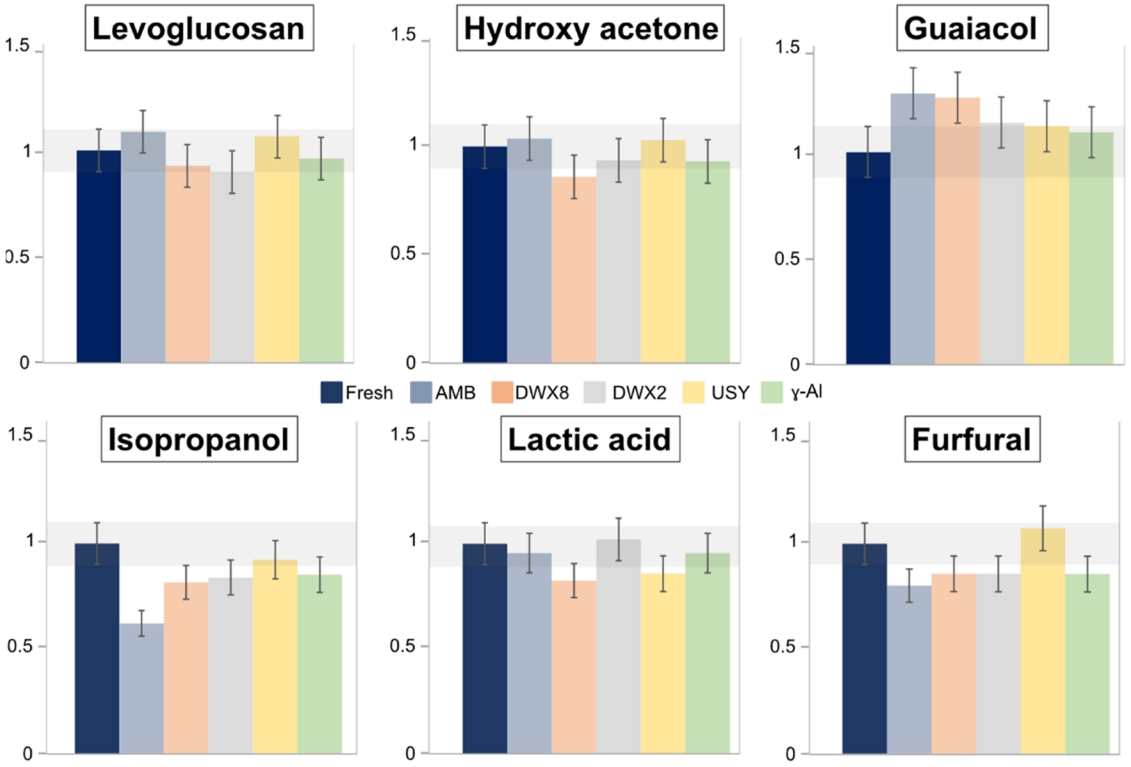

Figure 11. Semiquantification by GCxGC-MS using relative peak volumes normalized to the fresh oil of the compounds identified. Standard deviation of the instrument: 0.5−10.4%.

eutrophication in water. They found electrostatic interactions at low pH, where surface hydroxyls (that have higher Lewis acidity) form complexes with phosphorus by ligand-exchange reactions, and that this reaction depends on the type of alumina. Also, Islam et al.[52] found the adsorption of phosphate on aluminum oxides to be most successful at low pH, which for removal from the acidic FPBO is favorable. The SEM images in Figure 4 show that the resins were fractured likely due to the stirrer. A control experiment was performed using an inert, viscous liquid (hexadecane) of which the results are presented in Figure S2 in the Supporting Information. Fracturing was observed but not at all to the same extent as when using the FPBO, suggesting that the fracturing is due to a combination of the strongly acidic FPBO and the magnetic stirring. The fracturing caused by stirring/FPBO did not seem to affect the removal of the adsorbates negatively compared to USY and γ-Al_2O_3. Fracturing caused by the stirrer is an issue in laboratory conditions: in an industrial setting, the use of a continuous packed bed is preferable, which could avoid any attrition caused by the stirrer. Furthermore, the use of a solvent in a potential industrial setting could also be addressed here. Research on the upgrading of FPBO such as esterification (for reducing the acidity) involves addition of alcohol and is thereafter followed by azeotropic distillation.[53] A separation process such as this would thus be beneficial for solvent recycling.

Semiquantification of the pretreated FPBO was carried out using GCxGC-MS to examine whether the adsorbent experiment influences the chemical composition of the FPBO. The peak volumes were standardized against an internal standard and then normalized against the fresh sample, as shown in Figure 11. A selection of some typical compounds present in the pyrolysis oil were studied, namely, levoglucosan, hydroxy acetone, guaiacol, isopropanol, lactic acid, and furfural (Figure 11a−f, respectively). All of these compounds showed a relative peak volume greater than 2% of the total peak volume. After the sorbent experiments, the contents of levoglucosan, hydroxy acetone, lactic acid, and furfural were all within 10% of that in the fresh oil (marked in gray). However, for Amberlyst, there was a notable decrease in isopropanol and a slight increase in guaiacol. The resins are not known for the formation of phenolics or converting alcohols but rather the esterification of acids[48] or conversion from sugar to furan.[49] Moreover, the temperature during the sorption experiments was only 30 °C. It is therefore suggested that the lower amount of isopropanol in the case of Amberlyst is due to experimental deviations, considering the very complex chemical mixture of the FPBO. Each sorbent material employed in this study can be used as a catalyst or support material for a catalyst in the conversion of organic compounds but not at the low temperatures used in these sorbent experiments.[15,20,48,49] It can be concluded that there was no indication of changes in the chemical composition during the sorption experiments.

3.4. Mass Balance of Impurities and Reusability of Sorbents. Mass balances of Ca, Fe, K, Mg, and P were calculated by adding the initial impurities (in mg) and comparing them to the final content in the sorbents and the FPBO (Supporting Information, plotted in Figures S4−S6 and raw data in Tables S6−S8). A mass balance for all elements except P in γ-Al_2O_3 was found, while the masses in the Amberlyst experiments were not as balanced. It is likely that some of the Ca and Mg from Amberlyst and P from the γ-Al_2O_3 were washed off from the sorbents when rinsing the residual FPBO before the ICP analysis, resulting in a partial regeneration of the sorbent materials. As the properties of Amberlyst and γ-Al_2O_3 differ in many aspects, such as chemical

https://doi.org/10.1021/acs.energyfuels.3c02473
Energy Fuels 2024, 38, 414−425

structure and surface acidity, it is likely that they reacted differently to the final washing of the sorbents after filtration prior to ICP analysis. The results in this work are therefore focused on the contents in the bio-oil.

Finally, the reusage of Amberlyst at 5 wt % loading was evaluated (Figure 12), as the same Amberlyst sample was used

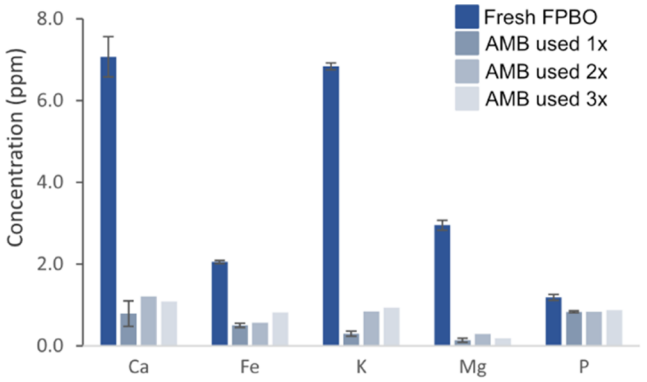

Figure 12. Concentration of elements Ca, Fe, K, Mg, and P in the FPBO after experiments with Amberlyst repeated 1−3 times.

and exposed to fresh FPBO three times. In general, the removal efficiency was quite similar for the three experiments, indicating that the Amberlyst was not saturated with the poison. However, for Fe and K, it was indicated that after three reuses, the concentration in the FPBO was higher than that after two reuses, suggesting that it is starting to become saturated; however, since the removal efficiency was still high, it is likely that there is more capacity left.

4. CONCLUSIONS

Fast pyrolysis bio-oil (FPBO) with typical characteristics, supplied by an industrial source, was pretreated at ambient conditions using strongly acidic ion-exchange resins, USY zeolite, and γ-Al_2O_3 with different surface acidities, sizes, and chemical structures with the aim of removing five specific inorganic impurities: Ca, K, Mg, Fe, and P. These inorganic impurities were measured using ICP-SFMS, which confirmed their removal by comparison to the initial amounts present. Both USY and the resins showed a similar degree of removal efficiency for the cationic metals. The strongly acidic ion-exchange resin Dowex 8 showed the highest percentage removal after experiments when compared to the initial concentration in the oil of Ca (>85% removal, detection limit met at 1 ppm), K (91%), Mg (>93% removal, detection limit met at 0.1 ppm), and Fe (>98% removal, detection limit was met at 0.02 ppm). γ-Al_2O_3 was inefficient for removing the cations, which can be explained by its lower Brønsted acid site density compared to that of the USY and the resins.

In the case of P, there was less removal with the more surface acidic sorbent types compared to γ-Al_2O_3, which removed P successfully (>85%, detection limit met at 0.1 ppm). Although γ-Al_2O_3 showed a lower capability of removing the cations in general, it nevertheless had a higher adsorption capacity for Ca than for the other cations. The previous study carried out on the removal of cations using strongly acidic resins suggested that the metals are present in the ionic form, which further explains the affinity of cations for the strongly acidic resins and USY. The anionic P was removed successfully only by γ-Al_2O_3, which had Lewis sites rather than strongly acidic Brønsted sites. GCxGC-MS analysis made before and after the experiments showed that the organic compounds of the FPBO were not affected by the sorbents, which is probably due to the mild ambient conditions of the experiments.

Avoiding HDO catalyst deactivation by the selective removal of inorganic impurities from bio-oils has the potential to enable more residual streams to be converted into pyrolysis oil and biofuels. Successful removal can be achieved under ambient conditions and with low initial concentrations of elements.

■ ASSOCIATED CONTENT

Supporting Information

The Supporting Information is available free of charge at https://pubs.acs.org/doi/10.1021/acs.energyfuels.3c02473.

Raw data and plots of repeated experiments and mass balances (PDF)

■ AUTHOR INFORMATION

Corresponding Author

Louise Olsson − *Chemical Engineering Division, Competence Centre for Catalysis, Chalmers University of Technology, Gothenburg 41296, Sweden;* orcid.org/0000-0002-8308-0784; Email: louise.olsson@chalmers.se

Authors

Emma Olsson Månsson − *Chemical Engineering Division, Competence Centre for Catalysis, Chalmers University of Technology, Gothenburg 41296, Sweden;* orcid.org/0000-0002-6600-4608

Abdenour Achour − *Chemical Engineering Division, Competence Centre for Catalysis, Chalmers University of Technology, Gothenburg 41296, Sweden*

Phuoc Hoang Ho − *Chemical Engineering Division, Competence Centre for Catalysis, Chalmers University of Technology, Gothenburg 41296, Sweden*

Prakhar Arora − *Preem AB, Gothenburg SE-417 26, Sweden*

Olov Öhrman − *Preem AB, Gothenburg SE-417 26, Sweden;* orcid.org/0000-0003-2324-4318

Derek Creaser − *Chemical Engineering Division, Competence Centre for Catalysis, Chalmers University of Technology, Gothenburg 41296, Sweden;* orcid.org/0000-0002-5569-5706

Complete contact information is available at: https://pubs.acs.org/10.1021/acs.energyfuels.3c02473

Notes

The authors declare no competing financial interest.

■ ACKNOWLEDGMENTS

This work was performed at the Chemical Engineering and Competence Centre for Catalysis at the Chalmers University of Technology in Gothenburg, in collaboration with Preem. The Chalmers Materials Analysis Laboratory (CMAL) is thanked for the SEM images. The Swedish Energy Agency and Preem are thanked for funding the project (No. P49670-1).

■ NOMENCLATURE

AMB =Amberlyst 15 resin
BET =Brunauer−Emmett−Teller
C_0 =initial concentration (ppm) (eq 5)
C_f =final concentration (ppm) (eq 5)

DL =detection limit
DWX =Dowex resin
EtOH =ethanol
FPBO =fast pyrolysis bio-oil
γ-Al =γ-aluminum oxide
γ-Al_2O_3 =γ-aluminum oxide
GCxGC-MS =two-dimensional gas chromatography coupled with mass spectrometry
GHG =greenhouse gases
HDO =hydrodeoxygenation
HHV =higher heating value
HVO =hydrogenated vegetable oils
ICP-SFMS =inductively coupled plasma with sector field mass spectrometry
M_{KOH} =mass of KOH (eq 1)
NH_3-TPD =ammonia temperature-programmed desorption
N_{KOH} =moles of KOH (eq 1)
PFA =perfluoroalkoxy
RED II =renewable energy directive 2
TAN =total acid number
TGA =thermogravimetric analysis
USY =zeolite Y
V_{KOH} =volume of KOH (eq 1)
$m_{j,sorbent,exp}$ =absolute mass of element j in sorbent after experiment (eq 3)
c_j =concentration of element j measured by ICP (eqs 3 and 4)
$m_{sorbent,exp}$ =absolute mass of sorbent used in the experiment (eq 3)
$m_{j,oil,exp}$ =absolute mass of element j in oil after experiment (eq 4)
$m_{oil,exp}$ =absolute mass of oil used in the experiment (eq 4)

REFERENCES

(1) *Renewable Energy Progress Report*; European Comission: Brussels, 2019.
(2) Huber, G. W.; Iborra, S.; Corma, A. Synthesis of transportation fuels from biomass: Chemistry, catalysts, and engineering. *Chem. Rev.* **2006**, *106* (9), 4044−4098 Review.
(3) Chang, W. R.; Hwang, J. J.; Wu, W. Environmental impact and sustainability study on biofuels for transportation applications. *Renewable Sustainable Energy Rev.* **2017**, *67*, 277−288.
(4) Brännström, H.; Kumar, H.; Alen, R. Current and Potential Biofuel Production from Plant Oils. *BioEnergy Res.* **2018**, *11* (3), 592−613, DOI: 10.1007/s12155-018-9923-2.
(5) Cashman, S. A.; Moran, K. M.; Gaglione, A. G. Greenhouse Gas and Energy Life Cycle Assessment of Pine Chemicals Derived from Crude Tall Oil and Their Substitutes. *J. Ind. Ecol.* **2016**, *20* (5), 1108−1121, DOI: 10.1111/jiec.12370.
(6) Eschenbacher, A.; Saraeian, A.; Jensen, P. A.; Shanks, B. H.; Li, C.; Duus, JØ.; Smitshuysen, T. E. L.; Damsgaard, C. D.; Hansen, A. B.; Kling, K. I.; et al. Deoxygenation of wheat straw fast pyrolysis vapors over Na-Al2O3 catalyst for production of bio-oil with low acidity. *Chem. Eng. J.* **2020**, *394*, No. 124878.
(7) Zhang, Y.; Xie, X.; Zhao, J.; Wei, X. The alkali metal occurrence characteristics and its release and conversion during wheat straw pyrolysis. *Renewable Energy* **2020**, *151*, 255−262.
(8) Charis, G.; Danha, G.; Muzenda, E. Optimizing Yield and Quality of Bio-Oil: A Comparative Study ofAcacia tortilisand Pine Dust. *Processes* **2020**, *8* (5), No. 551, DOI: 10.3390/pr8050551.
(9) Garba, M. U.; Musa, U.; Olugbenga, A. G.; Mohammad, Y. S.; Yahaya, M.; Ibrahim, A. A. Catalytic upgrading of bio-oil from bagasse: Thermogravimetric analysis and fixed bed pyrolysis. *Beni-Suef Univ. J. Basic Appl. Sci.* **2018**, *7* (4), 776−781.
(10) Cheng, S.; Wei, L.; Zhao, X.; Julson, J. Application, Deactivation, and Regeneration of Heterogeneous Catalysts in Bio-Oil Upgrading. *Catalysts* **2016**, *6*, No. 195, DOI: 10.3390/catal6120195.
(11) Bezergianni, S.; Dimitriadis, A.; Kikhtyanin, O.; Kubicka, D. Refinery co-processing of renewable feeds. *Prog. Energy Combust. Sci.* **2018**, *68*, 29−64.
(12) Oasmaa, A.; Lehto, J.; Solantausta, Y.; Kallio, S. Historical Review on VTT Fast Pyrolysis Bio-oil Production and Upgrading. *Energy Fuels* **2021**, *35* (7), 5683−5695.
(13) Oasmaa, A.; Czernik, S. Fuel Oil Quality of Biomass Pyrolysis OilsState of the Art for the End Users. *Energy Fuels* **1999**, *13* (4), 914−921.
(14) Olarte, M. V.; Zacher, A. H.; Padmaperuma, A. B.; Burton, S. D.; Job, H. M.; Lemmon, T. L.; Swita, M. S.; Rotness, L. J.; Neuenschwander, G. N.; Frye, J. G.; Elliott, D. C. Stabilization of Softwood-Derived Pyrolysis Oils for Continuous Bio-oil Hydroprocessing. *Top. Catal.* **2016**, *59* (1), 55−64.
(15) Grilc, M.; Likozar, B.; Levec, J. Simultaneous Liquefaction and Hydrodeoxygenation of Lignocellulosic Biomass over NiMo/Al2O3, Pd/Al2O3, and Zeolite Y Catalysts in Hydrogen Donor Solvents. *ChemCatChem* **2016**, *8* (1), 180−191.
(16) Benés, M.; Bilbao, R.; Santos, J. M.; Melo, J. A.; Wisniewski, A.; Fonts, I. Hydrodeoxygenation of Lignocellulosic Fast Pyrolysis Bio-Oil: Characterization of the Products and Effect of the Catalyst Loading Ratio. *Energy Fuels* **2019**, *33* (5), 4272−4286, DOI: 10.1021/acs.energyfuels.9b00265.
(17) Routray, K.; Barnett, K. J.; Huber, G. W. Hydrodeoxygenation of Pyrolysis Oils. *Energy Technol.* **2017**, *5* (1), 80−93.
(18) Žula, M.; Grilc, M.; Likozar, B. Hydrocracking, hydrogenation and hydro-deoxygenation of fatty acids, esters and glycerides: Mechanisms, kinetics and transport phenomena. *Chem. Eng. J.* **2022**, *444*, No. 136564.
(19) Kostyniuk, A.; Bajec, D.; Likozar, B. Hydrocracking, hydrogenation and isomerization of model biomass tar in a packed bed reactor over bimetallic NiMo zeolite catalysts: Tailoring structure/acidity. *Appl. Catal., A* **2021**, *612*, No. 118004.
(20) Arora, P.; Ojagh, H.; Woo, J.; Grennfelt, E. L.; Olsson, L.; Creaser, D. Investigating the effect of Fe as a poison for catalytic HDO over sulfided NiMo alumina catalysts. *Appl. Catal., B* **2018**, *227*, 240−251.
(21) Arora, P.; Abdolahi, H.; Cheah, Y. W.; Salam, M. A.; Grennfelt, E. L.; Rådberg, H.; Creaser, D.; Olsson, L. The role of catalyst poisons during hydrodeoxygenation of renewable oils. *Catal. Today* **2021**, *367*, 28−42.
(22) Nadeina, K. A.; Kazakov, M. O.; Kovalskaya, A. A.; Danilevich, V. V.; Klimov, O. V.; Danilova, I. G.; Khabibulin, D. F.; Gerasimov, E. Y.; Prosvirin, I. P.; Ushakov, V. A.; et al. Guard bed catalysts for silicon removal during hydrotreating of middle distillates. *Catal. Today* **2019**, *329*, 53−62.
(23) Hart, A.; Shah, A.; Leeke, G.; Greaves, M.; Wood, J. Optimization of the CAPRI Process for Heavy Oil Upgrading: Effect of Hydrogen and Guard Bed. *Ind. Eng. Chem. Res.* **2013**, *52* (44), 15394−15406.
(24) Boldushevskii, R. E.; Guseva, A. I.; Vinogradova, N. Y.; Naranov, E. R.; Maksimov, A. L.; Nikul'shin, P. A. Evaluation of the Hydrodesulfurization Activity in Development of Catalysts for Demetallization of Heavy Petroleum Feedstock. *Russ. J. Appl. Chem.* **2018**, *91* (12), 2046−2051 Article.
(25) Danmaliki, G. I.; Saleh, T. A. Effects of bimetallic Ce/Fe nanoparticles on the desulfurization of thiophenes using activated carbon. *Chem. Eng. J.* **2017**, *307*, 914−927.
(26) Burakov, A. E.; Galunin, E. V.; Burakova, I. V.; Kucherova, A. E.; Agarwal, S.; Tkachev, A. G.; Gupta, V. K. Adsorption of heavy metals on conventional and nanostructured materials for wastewater treatment purposes: A review. *Ecotoxicol. Environ. Saf.* **2018**, *148*, 702−712.
(27) Hua, M.; Zhang, S. J.; Pan, B. C.; Zhang, W. M.; Lv, L.; Zhang, Q. X. Heavy metal removal from water/wastewater by nanosized metal oxides: A review. *J. Hazard. Mater.* **2012**, *211-212*, 317−331.

https://doi.org/10.1021/acs.energyfuels.3c02473
Energy Fuels 2024, 38, 414−425

(28) López, A.; de Marco, I.; Caballero, B. M.; Laresgoiti, M. F.; Adrados, A. Dechlorination of fuels in pyrolysis of PVC containing plastic wastes. *Fuel Process. Technol.* **2011**, *92* (2), 253−260.
(29) Osio-Norgaard, J.; Srubar, W. V. Zeolite Adsorption of Chloride from a Synthetic Alkali-Activated Cement Pore Solution. *Materials* **2019**, *12* (12), No. 2019, DOI: 10.3390/ma12122019.
(30) Chakraborty, R.; Asthana, A.; Singh, A. K.; Jain, B.; Susan, A. B. Adsorption of heavy metal ions by various low-cost adsorbents: a review. *Int. J. Environ. Anal. Chem.* **2022**, *102* (2), 342−379.
(31) Kabir, G.; Hameed, B. H. Recent progress on catalytic pyrolysis of lignocellulosic biomass to high-grade bio-oil and bio-chemicals. *Renewable Sustainable Energy Rev.* **2017**, *70*, 945−967.
(32) Zhou, G.; Roby, S. Study on the Removal of Metals from Pyrolysis Oil with Ion-Exchange Resins at Ambient Conditions. *Energy Fuels* **2016**, *30* (2), 1002−1005.
(33) Church, A. L.; Hu, M. Z.; Lee, S.-J.; Wang, H.; Liu, J. Selective adsorption removal of carbonyl molecular foulants from real fast pyrolysis bio-oils. *Biomass Bioenergy* **2020**, *136*, No. 105522.
(34) Agblevor, F. A. In *Rapid Method for the Determination of Total Acid Number (TAN) of Bio Oils*, AIChE Annual Meeting; AIChE: Salt Lake City, UT, 2010.
(35) Shafaghat, H.; Linderberg, M.; Janosik, T.; Hedberg, M.; Wiinikka, H.; Sandstrom, L.; Johansson, A. C. Enhanced Biofuel Production via Catalytic Hydropyrolysis and Hydro-Coprocessing. *Energy Fuels* **2022**, *36* (1), 450−462.
(36) Elliott, D. C.; Oasmaa, A.; Preto, F.; Meier, D.; Bridgwater, A. V. Results of the IEA Round Robin on Viscosity and Stability of Fast Pyrolysis Bio-oils. *Energy Fuels* **2012**, *26* (6), 3769−3776.
(37) Roby, S. H.; Dutta, M.; Zhu, Y. Y.; Pathiparampil, A. Development of an Acid Titration for Fast Pyrolysis Oil. *Energy Fuels* **2015**, *29* (2), 858−862.
(38) Oasmaa, A.; Elliott, D. C.; Korhonen, J. Acidity of Biomass Fast Pyrolysis Bio-oils. *Energy Fuels* **2010**, *24* (12), 6548−6554.
(39) Hakeem, I. G.; Halder, P.; Marzbali, M. H.; Patel, S.; Kundu, S.; Paz-Ferreiro, J.; Surapaneni, A.; Shah, K. Research progress on levoglucosan production via pyrolysis of lignocellulosic biomass and its effective recovery from bio-oil. *J. Environ. Chem. Eng.* **2021**, *9* (4), No. 105614.
(40) Beceiro, J. L.; Díaz-Díaz, A.; Álvarez-García, A.; Tarrío-Saavedra, J.; Naya, S.; Artiaga, R. The Complexity of Lignin Thermal Degradation in the Isothermal Context. *Processes* **2021**, *9*, No. 1154, DOI: 10.3390/pr9071154.
(41) Staš, M.; Chudoba, J.; Kubička, D.; Blažek, J.; Pospíšil, M. Petroleomic Characterization of Pyrolysis Bio-oils: A Review. *Energy Fuels* **2017**, *31* (10), 10283−10299.
(42) Staš, M.; Auersvald, M.; Kejla, L.; Vrtiška, D.; Kroufek, J.; Kubička, D. Quantitative analysis of pyrolysis bio-oils: A review. *TrAC, Trends Anal. Chem.* **2020**, *126*, No. 115857. Review.
(43) Janosik, T.; Nilsson, A. N.; Hallgren, A. C.; Hedberg, M.; Bernlind, C.; Radberg, H.; Ahlsen, L.; Arora, P.; Öhrman, O. G. W. Derivatizing of Fast Pyrolysis Bio-Oil and Coprocessing in Fixed Bed Hydrotreater. *Energy Fuels* **2022**, *36* (15), 8274−8287.
(44) Staš, M.; Auersvald, M.; Vozka, P. Two-Dimensional Gas Chromatography Characterization of Pyrolysis Bio-oils: A Review. *Energy Fuels* **2021**, *35* (10), 8541−8557.
(45) Marsman, J. H.; Wildschut, J.; Evers, P.; de Koning, S.; Heeres, H. J. Identification and classification of components in flash pyrolysis oil and hydrodeoxygenated oils by two-dimensional gas chromatography and time-of-flight mass spectrometry. *J. Chromatogr. A* **2008**, *1188* (1), 17−25.
(46) Djokic, M. R.; Dijkmans, T.; Yildiz, G.; Prins, W.; Van Geem, K. M. Quantitative analysis of crude and stabilized bio-oils by comprehensive two-dimensional gas-chromatography. *J. Chromatogr. A* **2012**, *1257*, 131−140.
(47) Limlamthong, M.; Yip, A. C. K. Recent advances in zeolite-encapsulated metal catalysts: A suitable catalyst design for catalytic biomass conversion. *Bioresour. Technol.* **2020**, *297*, No. 122488. Review.
(48) Kuzminska, M.; Backov, R.; Gaigneaux, E. M. Behavior of cation-exchange resins employed as heterogeneous catalysts for esterification of oleic acid with trimethylolpropane. *Appl. Catal., A* **2015**, *504*, 11−16.
(49) Tempelman, C.; Jacobs, U.; Hut, T.; de Pina, E. P.; van Munster, M.; Cherkasov, N.; Degirmenci, V. Sn exchanged acidic ion exchange resin for the stable and continuous production of 5-HMF from glucose at low temperature. *Appl. Catal., A* **2019**, *588*, No. 117267. Article.
(50) Ojagh, H.; Creaser, D.; Salam, M. A.; Grennfelt, E. L.; Olsson, L. Hydroconversion of abietic acid into value-added fuel components over sulfided NiMo catalysts with varying support acidity. *Fuel Process. Technol.* **2019**, *190*, 55−66.
(51) Yang, X. F.; Wang, D. S.; Sun, Z. X.; Tang, H. X. Adsorption of phosphate at the aluminum (hydr)oxides-water interface: Role of the surface acid-base properties. Colloids and Surfaces a- Physicochemical and Engineering Aspects. *Colloids Surf., A* **2007**, *297*, 84−90.
(52) Islam, Md. A.; Morton, D. W.; Johnson, B. B.; Pramanik, B. K.; Mainali, B.; Angove, M. J. Metal ion and contaminant sorption onto aluminium oxide-based materials: A review and future research. *J. Environ. Chem. Eng.* **2018**, *6*, 6853−6869.
(53) Sundqvist, T.; Oasmaa, A.; Koskinen, A. Upgrading Fast Pyrolysis Bio-Oil Quality by Esterification and Azeotropic Water Removal. *Energy Fuels* **2015**, *29* (4), 2527−2534.

https://doi.org/10.1021/acs.energyfuels.3c02473
Energy Fuels 2024, 38, 414−425